

Original article

DOI: <https://doi.org/10.18721/JPM.16312>

AN ANTIPLANE CRACK EMERGING FROM THE TOP OF A SECTIONAL FUNCTIONAL GRADIENT WEDGE

V. V. Tikhomirov✉

Peter the Great St. Petersburg Polytechnic University, St. Petersburg, Russia

✉ victikh@mail.ru

Abstract. In the paper, the problem on an interface longitudinal shear crack located between two functionally graded wedge-shaped regions and emerging from their common vertex has been considered. The shear modules of the materials are quadratic functions of the polar angle. This kind of functional inhomogeneity made it possible to express all the components of the elastic field through a single harmonic function. Using the Mellin integral transform, the problem was reduced to the Wiener – Hopf scalar equation, for which an exact solution was obtained. The influence of gradients of elastic properties of materials and geometric parameters of the structure on the stress intensity factor was studied.

Keywords: functionally graded wedge, interface crack of longitudinal shear, stress intensity factor

Citation: Tikhomirov V. V., An antiplane crack emerging from the top of a sectional functional gradient wedge, St. Petersburg State Polytechnical University Journal. Physics and Mathematics. 16 (3) (2023) 150–159. DOI: <https://doi.org/10.18721/JPM.16312>

This is an open access article under the CC BY-NC 4.0 license (<https://creativecommons.org/licenses/by-nc/4.0/>)

Научная статья

УДК 539.3

DOI: <https://doi.org/10.18721/JPM.16312>

АНТИПЛОСКАЯ ТРЕЩИНА, ВЫХОДЯЩАЯ ИЗ ВЕРШИНЫ СОСТАВНОГО ФУНКЦИОНАЛЬНО-ГРАДИЕНТНОГО КЛИНА

В. В. Тихомиров✉

Санкт-Петербургский политехнический университет Петра Великого, Санкт-Петербург, Россия

✉ victikh@mail.ru

Аннотация. Рассматривается задача об интерфейсной трещине продольного сдвига, расположенной между двумя функционально-градиентными клиновидными областями и выходящей из их общей вершины. Модули сдвига материалов областей являются квадратичными функциями полярного угла. Такой вид функциональной неоднородности позволяет выразить все компоненты упругого поля через одну гармоническую функцию. С помощью интегрального преобразования Меллина проблема сведена к скалярному уравнению Винера – Хопфа, для которого получено точное решение. Изучено влияние градиентов упругих свойств материалов и геометрических параметров структуры на коэффициент интенсивности напряжений в вершине трещины.

Ключевые слова: функционально-градиентный клин, интерфейсная трещина продольного сдвига, коэффициент интенсивности напряжений

Ссылка для цитирования: Тихомиров В. В. Антиплоская трещина, выходящая из вершины составного функционально-градиентного клина // Научно-технические ведомости СПбГПУ. Физико-математические науки. 2023. Т. 16. № 3. С. 150–159. DOI: <https://doi.org/10.18721/JPM.16312>

Статья открытого доступа, распространяемая по лицензии CC BY-NC 4.0 (<https://creativecommons.org/licenses/by-nc/4.0/>)



Introduction

The corner points of elastic structures are zones of increased stress concentration, consequently acting as sites where cracks initiate and propagate. Cracks initiating from the vertex of isotropic, anisotropic, and composite wedges have been considered in many studies within the framework of the antiplane problem [1–5]. However, similar analysis has not been carried out yet for wedge-shaped regions consisting of materials with gradient properties.

Functionally graded materials (FGM) are composites whose mechanical properties vary continuously over the volume. Used as coatings, they provide protection from thermally or chemically aggressive environments. Common types of mechanical damage to thin coatings are cracking and delamination. Fracture of layered gradient coatings with an interfacial crack or with a crack perpendicular to the interface between has been studied, for example, in [6, 7]. Gradient materials used as interfacial regions allow for continuous variation of the material properties, thus increasing the adhesive strength of heterogeneous materials [8]. Analysis of a wedge-shaped structure with transition FGM was performed in [9].

The studies by Jin and Batra [10] confirmed that elastic fields near the tip of a crack located in FGM are similar to the fields in a homogeneous material if the elastic moduli are continuous and piecewise continuously differentiable. Linear or exponential dependences on coordinates are typically used for elastic moduli in analysis of FGMs with crack defects, providing analytical solutions to equilibrium equations. A quadratic dependence of the shear modulus on the polar angle was proposed in an earlier study [13] for gradient material, allowing to express all the components of the elastic field in terms of a single harmonic function under the conditions of an antiplane problem. This dependence of the elastic modulus was used in [11] to analyze a composite gradient wedge weakened by a semi-infinite crack.

This paper considers a stress-strain state of a composite functionally graded wedge with a crack propagating from its vertex. The effects of increasing or decreasing stress intensity coefficient (SIF) at the crack tip are considered depending on the composition of materials, compared with the homogeneous case.

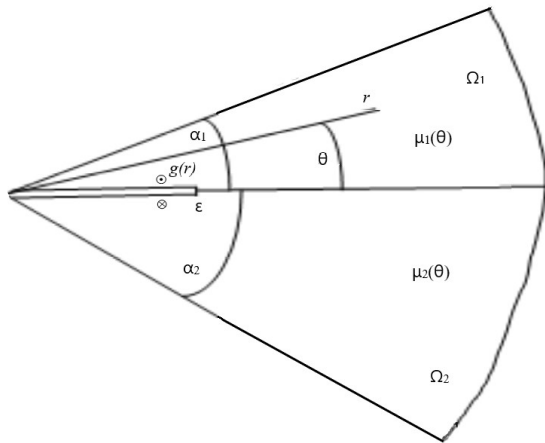


Fig. 1. Composite functionally graded wedge with interfacial longitudinal-shear crack propagating from its vertex: $\mu_1(\theta)$, $\mu_2(\theta)$ are the shear moduli of FGM materials in the regions Ω_1 and Ω_2 ; α_1 , α_2 , θ , r , ε are the geometric parameters; $g(r)$ is the self-balanced load applied to the edges of the crack

Problem statement

Consider a composite wedge containing an interfacial antiplane crack of length ε initiating from its vertex (Fig. 1).

Materials of the subdomains are designated as

$$\Omega_1 = \{(r, \theta) : 0 \leq r < \infty, 0 \leq \theta \leq \alpha_1\},$$

$$\Omega_2 = \{(r, \theta) : 0 \leq r < \infty, -\alpha_2 \leq \theta \leq 0\}$$

(r, θ are polar coordinates) and are assumed to be functionally graded.

The shear moduli of the materials are functions of the polar angle and take the values $\tilde{\mu}_1$ and $\tilde{\mu}_3$ at the interfaces $\theta = \alpha_1$ and $\theta = \alpha_2$, respectively. The shear moduli of the materials have the same magnitude, equal to $\tilde{\mu}_2$, at the interface. The contact of materials outside the crack is assumed to be perfect. The self-balanced load $g(r)$ is applied to the edges of crack.

If the shear moduli of the materials of regions Ω_j depend on the polar angle, the equilibrium equations have the form

$$\frac{\partial^2 w_j}{\partial r^2} + \frac{1}{r^2} \frac{\partial^2 w_j}{\partial \theta^2} + \frac{1}{r} \frac{\partial w_j}{\partial r} + \frac{1}{\mu_j(\theta)r^2} \frac{d\mu_j}{d\theta} \frac{\partial w_j}{\partial \theta} = 0, \tag{1}$$

and the stresses are expressed in terms of displacements w_j by the formulas:

$$\tau_{\theta z_j} = \frac{\mu_j}{r} \frac{\partial w_j}{\partial \theta}, \quad \tau_{r z_j} = \mu_j \frac{\partial w_j}{\partial r} \quad (j = 1, 2). \quad (2)$$

We adopt quadratic dependences on the angular coordinate for the shear moduli of materials:

$$\mu_j(\theta) = (a_j \theta + b_j)^2,$$

whose coefficients, determined by the values at the interfaces, take the form

$$a_1 = (\sqrt{\tilde{\mu}_1} - \sqrt{\tilde{\mu}_2})/\alpha_1, \quad a_2 = (\sqrt{\tilde{\mu}_3} - \sqrt{\tilde{\mu}_2})/\alpha_2, \quad b_1 = -b_2 = \sqrt{\tilde{\mu}_2}.$$

If we assume that the displacements in the regions Ω_j can be represented as

$$w_j(r, \theta) = \frac{1}{a_j \theta + b_j} \tilde{w}_j(r, \theta), \quad (3)$$

then it follows from Eqs. (1) that the functions $\tilde{w}_j(r, \theta)$ are harmonic, and the stresses are defined by the formulas

$$w_j(r, \theta) = \frac{1}{a_j \theta + b_j} \tilde{w}_j(r, \theta), \quad (4)$$

$$\tau_{r z_j} = (a_j \theta + b_j) \frac{\partial \tilde{w}_j}{\partial r}.$$

The components of elastic fields (3), (4) must satisfy mixed conditions at the interface between materials and the no-stress condition at the outer edges of the composite:

$$\begin{aligned} \tau_{\theta z_1}(r, +0) &= \tau_{\theta z_2}(r, -0) = g(r) \quad (0 \leq r < \varepsilon), \\ \tau_{\theta z_1}(r, +0) &= \tau_{\theta z_2}(r, -0), \quad w_1(r, +0) = w_2(r, -0) \quad (\varepsilon < r < \infty), \\ \tau_{\theta z_1}(r, \alpha_1) &= 0, \quad \tau_{\theta z_2}(r, -\alpha_2) = 0 \quad (0 \leq r < \infty). \end{aligned} \quad (5)$$

Reducing the problem to the Wiener–Hopf equation and its solution

Applying the integral Mellin transform, we obtain the following representations for displacements and stresses:

$$w_j(r, \theta) = \frac{1}{2\pi i} \int_L W_j(p, \theta) r^{-p} dp, \quad (6)$$

$$\tau_{\theta z_j}(r, \theta) = \frac{1}{2\pi i} \int_L T_{\theta z_j}(p, \theta) r^{-p-1} dp,$$

where the transforms, according to Eqs. (3) and (4), are expressed as

$$\begin{aligned} W_j(p, \theta) &= [A_j(p) \sin p\theta + B_j(p) \cos p\theta] / (a_j \theta + b_j), \\ T_{\theta z_j}(p, \theta) &= -a_j [A_j(p) \sin p\theta + B_j(p) \cos p\theta] + \\ &+ (a_j \theta + b_j) p [A_j(p) \cos p\theta - B_j(p) \sin p\theta]. \end{aligned}$$



In accordance with the regularity conditions, the integration path L in Eqs. (6) is located parallel to the imaginary axis in the strip $-\delta_1 < \operatorname{Re} p < \delta_2$ ($\delta_1, \delta_2 > 0$). The quantities depending on the integral transformation parameter, $A_j(p)$ and $B_j(p)$ ($j = 1, 2$) are determined from the conditions (5).

We introduce the following functions:

$$\begin{aligned}
 U_+(p) &= \int_0^1 \frac{\partial}{\partial \rho} [w_1(\varepsilon \rho, +0) - w_2(\varepsilon \rho, -0)] \rho^p d\rho, \\
 T_-(p) &= \int_1^\infty \tau_{\theta z 1}(\varepsilon \rho, +0) \rho^p d\rho, G_+(p) = \int_0^1 g(\varepsilon \rho) \rho^p d\rho.
 \end{aligned} \tag{7}$$

In this case, $W_+(p)$ and $G_+(p)$ are regular and have no zeros in the right half-plane Ω_+ of the path L , and $T_-(p)$ in the left half-plane Ω_- [12]. Expressing the quantities $A_j(p)$ and $B_j(p)$ in terms of functions (7) under Mellin-transformed boundary conditions (5), we arrive at the scalar Wiener–Hopf equation:

$$F(p)[T_-(p) + G_+(p)] + \tilde{\mu}_2 \varepsilon^{-1} U_+(p) = 0 \quad (p \in L), \tag{8}$$

where

$$F(p) = \operatorname{ctg}(\alpha_1 p) \frac{v_1(\alpha_1 p)}{u_1(\alpha_1 p)} + \operatorname{ctg}(\alpha_2 p) \frac{v_2(\alpha_2 p)}{u_2(\alpha_2 p)}, \tag{9}$$

$$u_j(x) = 1 + m_j^{-1} (m_j - 1)^2 x^{-2} [1 - x \operatorname{ctg}(x)], \tag{10}$$

$$v_j(x) = 1 + (m_j - 1)x^{-1} \operatorname{tg}(x) \quad (j = 1, 2),$$

$$m_1 = \sqrt{\tilde{\mu}_2 / \tilde{\mu}_1}, \quad m_2 = \sqrt{\tilde{\mu}_2 / \tilde{\mu}_3},$$

$$\tilde{\mu}_1 = \mu_1(\alpha_1), \quad \tilde{\mu}_2 = \mu_1(0) = \mu_2(0), \quad \tilde{\mu}_3 = \mu_2(-\alpha_2).$$

Eqs. (10) include two dimensionless parameters m_j ($0 < m_j < \infty$) that characterize the relative shear stiffnesses of materials along the crack line with respect to materials at the outer faces of the wedge. The crack is located in the region of locally soft material if $0 < m_j < 1$, and in the region of locally rigid material if $1 < m_j < \infty$. The value $m_j = 1$ corresponds to a homogeneous material in the region Ω_j . In the case of a homogeneous wedge, when $m_1 = m_2 = 1$, we write the expression obtained in [13] for the coefficient in Eq. (8) from Eqs. (9) and (10). If $m_1 = m_2$, then the function $F(p)$ takes the form found in [11].

To factorize function (12), let us represent it in the following form:

$$F(p) = \frac{2}{p} K(p), \tag{11}$$

$$K(p) = X(p)\Phi(p), \quad X(p) = p \operatorname{ctg}(\alpha_1 p),$$

$$\Phi(p) = \frac{1}{2} F_1(p)F_2(p), \quad F_1(p) = \frac{v_1(\alpha_1 p)}{u_1(\alpha_1 p)},$$

$$F_2(p) = 1 + \operatorname{tg}(\alpha_1 p) \operatorname{ctg}(\alpha_2 p) \frac{u_1(\alpha_1 p)v_2(\alpha_2 p)}{u_2(\alpha_2 p)v_1(\alpha_1 p)}.$$

The function $\Phi(it)$ is continuous along the imaginary axis at $p = it$, it has no zeros and poles, its index is zero and it exponentially tends to unity at $t \rightarrow \infty$. Therefore, according to the calculations given in [12], we obtain:

$$\Phi(p) = \Phi_+(p)\Phi_-(p), \tag{12}$$

$$\Phi_{\pm}(p) = \exp \left[\mp \frac{1}{2\pi i} \int_L \frac{\ln \Phi(t)}{t-p} dt \right] \quad (p \notin L),$$

$$X(p) = X_+(p)X_-(p), \quad X_{\pm}(p) = \sqrt{\frac{\pi}{\alpha_1} \frac{\Gamma(1 \pm p\alpha_1/\pi)}{\Gamma(1/2 \pm p\alpha_1/\pi)}}.$$

Using Eqs. (11), (12) and applying Liouville's theorems [12], we obtain from Eq. (8):

$$X_-(p)\Phi_-(p)T_-(p) + Q_-(p) = -\frac{\tilde{\mu}_2 p}{2\varepsilon} U_+(p)X_+^{-1}(p)\Phi_+^{-1}(p) - Q_-(p) = J(p), \tag{13}$$

where

$$Q_{\pm}(p) = \mp \frac{1}{2\pi i} \int_L \frac{Q(t)}{t-p} dt, \quad Q(t) = \frac{t}{2} \Phi_+^{-1}(t)X_+^{-1}(t)F(t)G_+(t). \tag{14}$$

Evaluating the terms in equality (13) at $p \rightarrow \infty$, we can conclude that the single analytical function is constant:

$$J(p) = \text{const} = C.$$

This constant can be found from Eq. (13) for the $p = 0$.

Taking into account Eqs. (12) and (14), as well as the equality $T_-(0) = -G_+(0)$, which follows from the equilibrium equation of the region Ω_1 , we find that

$$C = -C_*G_+(0) + \frac{1}{4\pi i} \int_L X_+^{-1}(p)\Phi_+^{-1}(t)F(t)G_+(t)dt, \tag{15}$$

$$C_* = \Phi_-(0)X_-(0) = \left[\frac{3}{2\alpha_1\alpha_2} \left(\frac{\alpha_2 m_1^2}{m_1^2 + m_1 + 1} + \frac{\alpha_1 m_2^2}{m_2^2 + m_2 + 1} \right) \right]^{1/2}.$$

To calculate the integral in Eq. (15), we use Cauchy's residue theorem. The poles of the integrand, located in the half-plane Ω_+ (to the right of the path L), are the poles of $F(t)$; in view of Eq. (9), it is convenient to represent this function as

$$F(t) = m_1\alpha_1 t \frac{\tilde{v}_1(\alpha_1 t)}{\tilde{u}_1(\alpha_1 t)} + m_2\alpha_2 t \frac{\tilde{v}_2(\alpha_2 t)}{\tilde{u}_2(\alpha_2 t)}, \tag{16}$$

where

$$\tilde{v}_j(x) = x \cos x + (m_j - 1) \sin x, \quad x = \alpha_j t,$$

$$\tilde{u}_j(x) = m_j x^2 \sin x + (m_j - 1)^2 (\sin x - x \cos x) \quad (j = 1, 2). \tag{17}$$

It follows then that the poles of function (16) are determined by the positive roots of the equations $\tilde{u}(x) = 0$, located in the intervals $n\pi < x_{nj} < (n + 0.5)\pi$ ($n = 1, 2, \dots$).

We should note that there are two groups of poles: $t_{nj} = x_{nj}/\alpha_j$. We can prove that functions (17) do not have complex zeros. In addition, the poles in question are identical if m_j is substituted with m_j^{-1} .

As a result, we obtain from Eq. (19) that

$$C = -C_* G_+(0) - \frac{1}{2} \sqrt{\frac{\alpha_1}{\pi}} \sum_{j=1}^2 \sum_{n=1}^{\infty} a_{nj} G_+(t_{nj}), \quad (18)$$

where

$$a_{nj} = \frac{1}{\alpha_j} \frac{\Gamma(1/2 + \alpha_1 t_{nj}/\pi)}{\Gamma(1 + \alpha_1 t_{nj}/\pi)} \Phi_+^{-1}(t_{nj}) b(x_{nj}),$$

$$\Phi_+^{-1}(t_{nj}) = \exp \left[-\frac{t_{nj}}{\pi} \int_0^{\infty} \frac{\ln \Phi(i\xi)}{\xi^2 + t_{nj}^2} d\xi \right],$$

$$b(x_{nj}) = \frac{x_{nj} \cos x_{nj} + (m_j - 1) \sin x_{nj}}{x_{nj} \cos x_{nj} + (m_j + m_j^{-1}) \sin x_{nj}}.$$

Based on the Abel-type theorem [12], we conclude that the stress asymptote on the crack line at $r \rightarrow \varepsilon + 0$ has the form

$$\tau_{\theta z1}(r, 0) \sim C \sqrt{\frac{\varepsilon}{\pi}} \frac{1}{\sqrt{r - \varepsilon}}. \quad (19)$$

We define the stress intensity factor (SIF) at the crack tip by the formula

$$K_{III} = \lim_{r \rightarrow \varepsilon + 0} \sqrt{2\pi(r - \varepsilon)} \tau_{\theta z1}(r, 0).$$

Then, using asymptote (16), we obtain that

$$K_{III}(\alpha_1, \alpha_2, m_1, m_2, \varepsilon) = \sqrt{2\varepsilon} C. \quad (20)$$

Eqs. (18) and (20) determine the SIFs for various loading conditions of the crack edges with a self-balanced load based on finding the integral that defines the function $G_+(p)$ in Eqs. (7).

We assume that concentrated forces with the magnitude T_0 are applied to the edges of the crack at a distance r_0 from the vertex of the wedge. In this case,

$$g(r) = -T_0 \delta(r - r_0),$$

$$G_+(p) = -T_0 / \varepsilon (r_0 / \varepsilon)^p$$

($\delta(r - r_0)$ is the Dirac delta function).

Then, in accordance with Eqs. (18) and (20), we obtain the following representation for the SIF:

$$K_{III} = T_0 \sqrt{\frac{2}{\varepsilon}} \left[C_* + \frac{1}{2} \sqrt{\frac{\alpha_1}{\pi}} \sum_{j=1}^2 \sum_{n=1}^{\infty} a_{nj} \left(\frac{r_0}{\varepsilon} \right)^{t_{nj}} \right]. \quad (21)$$

To examine the effect from the gradient of the material, we introduce a normalized SIF of the form

$$N = K_{III} / K_{III}^0, \quad (22)$$

where K_{III}^0 is the SIF at the tip of the crack located in a homogeneous wedge.

The value of K_{III}^0 can be obtained from Eq. (21) by assuming $m_1 = m_2 = 1$. In this case, according to Eqs. (10),

$$u_j(x) = v_j(x) = 1 \quad (j = 1, 2).$$

Consequently, the functions included in representations (11) take the form

$$F_1(p) = 1, \quad F_2(p) = 1 + \operatorname{tg}(\alpha_1 p) \operatorname{ctg}(\alpha_2 p),$$

and the poles of the integrand in expression (15) are determined, in accordance with representation (9), by the formulas

$$t_{nj} = \pi n / \alpha_j \quad (n = 1, 2, \dots; j = 1, 2).$$

In particular, provided that the structure is geometrically symmetric, when $\alpha_1 = \alpha_2 = \alpha$, the series (21) is summed up, and the SIF in a homogeneous wedge has the form

$$K_{III}^0 = T_0 \sqrt{\frac{2}{\alpha \varepsilon}} \frac{\varepsilon^{\pi/(2\alpha)}}{\sqrt{\varepsilon^{\pi/\alpha} - r_0^{\pi/\alpha}}}.$$

Numerical results

SIF (21) depends on five parameters: the two opening angles α_1 and α_2 of the wedge-shaped regions Ω_1 and Ω_2 , the relative stiffnesses of these regions m_1 and m_2 , and the dimensionless parameter r_0/ε , which determines the positions of the points where forces are applied to the crack edges.

The effect of small values of the geometric parameter r_0/ε on SIF is very weak, increasing at r_0/ε close to unity when the convergence of the series in Eq. (21) worsens. The dependence of the normalized SIF (22) on the parameter r_0/ε , for example, in the case of a homogeneous region Ω_2 , is monotonically decreasing for $m_1 > 1$, and monotonically increasing for $m_1 < 1$. If $r_0/\varepsilon \ll 1$, series (21) do not make a significant contribution to the SIF, and its value in this case is determined by the quantity C_* . A similar situation also occurs in the case of small vertex angles of wedge-shaped regions, when α_1 and $\alpha_2 \ll 1$.

Fig. 2 shows the dependence of the normalized SIF (22) on the gradient properties of the material of the region Ω_1 for the case of a composite with a geometrically symmetric structure ($\alpha_1 = \alpha_2 = \alpha$) with a homogeneous region Ω_2 ($m_2 = 1$). If the material in the interfacial region has a lower shear stiffness compared to the outer boundary ($m_1 < 1$), then this leads to a decrease in SIF at all angles α ($N < 1$). Conversely, when a crack is located in a region containing a material

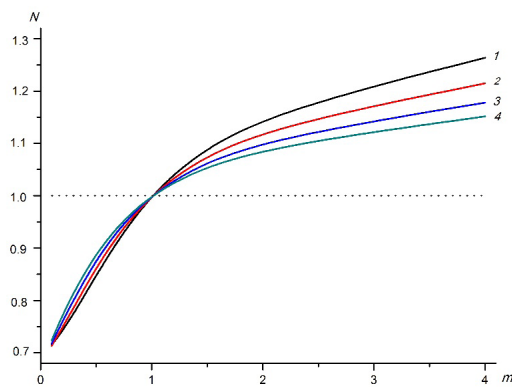


Fig. 2. Dependences of normalized SIF on relative shear stiffness m_1 of functionally graded region Ω_1 for a geometrically symmetric wedge and a homogeneous region Ω_2 at $\varepsilon/r_0 = 0.5$ for different angles $\alpha = \alpha_1 = \alpha_2$: $\pi/4$ (1); $\pi/2$ (2); $3\pi/4$ (3); π (4)



with high shear stiffness ($m_1 > 1$), an increase in SIF ($N > 1$) occurs, compared with the homogeneous case. At the same time, the effects from increasing and decreasing the normalized SIF become more pronounced with a decrease in the opening angles of the structure.

A similar situation occurs in the case of a composite with an asymmetrical structure. For example, SIF exhibits this behavior for a homogeneous region Ω_2 , shaped as a quarter-plane and any values of the angle within $0 < \alpha_1 \leq 3\pi/2$ (Fig. 3). The effect of the material gradient of the region Ω_1 on SIF becomes particularly pronounced in the case of thin wedge-shaped coatings, when the angle α_1 is sufficiently small.

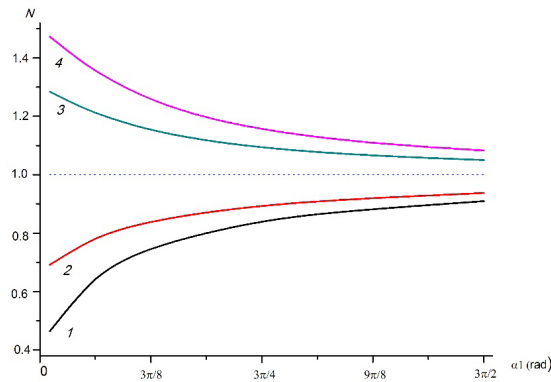


Fig. 3. Dependences of normalized KIN on angle α_1 of functionally graded region Ω_1 and homogeneous region Ω_2 shaped as a quarter plane at $\varepsilon/r_0 = 0.5$ for different values of parameter m_1 : 0.25 (1); 0.50 (2); 2.00 (3); 4.00 (4)

The variation in the SIF at the crack tip depending on the gradients of shear moduli in both materials is considered for a composite half-plane for angles $\alpha_1 = \alpha_2 = \pi/2$. In contrast to the case of homogeneous material in the region Ω_2 , when $m_2 = 1$, the situation is not as clear as before. In general, the presence of a shear modulus gradient in this region causes a decrease in the SIF at $m_2 < 1$ (see curves 1 and 2 in Fig. 4) and the increase in SIF at $m_2 > 1$ (curves 4 and 5) for any values of the parameter m_1 . However, the gradient properties of the material in the region Ω_2 can produce values $N > 1$ even in the case of a sufficiently small relative stiffness $m_1 < 1$ for $m_2 > 1$ (curves 4 and 5). Furthermore, the values of the parameter $m_2 < 1$ (curves 1 and 2) can result in normalized SIF values not exceeding unity in a certain range of relative shear stiffnesses when $m_1 > 1$.

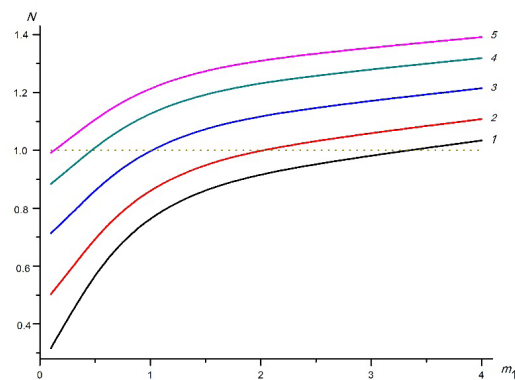


Fig. 4. Dependences of normalized SIF on relative shear stiffness m_1 at $\varepsilon/r_0 = 0.5$ in the case of a functionally graded half-plane formed by wedge-shaped regions with angles $\alpha_1 = \alpha_2 = \pi/2$, for different values of parameter m_2 : 0.25 (1); 0.50 (2); 1.00 (3); 2.00 (4); 4.00 (5)

Conclusion

We used the integral Mellin transform and the Wiener–Hopf method to obtain an exact solution to the equilibrium problem of a functionally graded composite wedge weakened by an interfacial crack under longitudinal shear initiating from its vertex. The edges of the crack were loaded with self-balanced concentrated forces. The shear moduli of the materials comprising the wedge between two wedge-shaped regions are assumed to depend quadratically on the angular coordinate and take the values set at the interface and the inner edges of the wedge. This functional dependence allows to express all the components of elastic fields in these regions in terms of harmonic functions.

We analyzed the influence of the geometric and stiffness parameters of the composite on the magnitude of the stress intensity coefficient (SIF) at the tip of the crack. Evidently, the gradient properties of materials can significantly affect this quantity. In the case when the crack is located in a region relatively softer than the regions near its edges, the SIF is significantly decreased compared to its value in a homogeneous material. Conversely, an increase in the stiffness of the materials in the interfacial region leads to an increase in the SIF compared to the homogeneous case.

The approach proposed in the paper can also be applied in the case when the shear moduli of materials have a jump along the crack line.

REFERENCES

1. **Wu X., Dzenis Y., Zou W.**, Screw dislocation interacting with an interfacial edge crack between two bonded piezoelectric wedges, *Int. J. Fract.* 117 (3) (2002) 9–14.
2. **Beom H. G., Jang H. S.**, A wedge crack in an anisotropic material under antiplane shear, *Int. J. Eng. Sci.* 49 (9) (2011) Pp. 867–880.
3. **Beom H. G., Jang H. S.**, A crack emanating from a wedge in dissimilar anisotropic materials under antiplane shear, *Int. J. Fract.* 177 (2) (2012) 191–198.
4. **Beom H. G., Jang H. S.**, Interfacial wedge cracks in dissimilar anisotropic materials under antiplane shear, *Int. J. Eng. Sci.* 56 (1) (2012) Pp. 49–62.
5. **Tikhomirov V. V.**, The exact solution of the problem on a crack emerging from the top of two dissimilar wedge, *St. Petersburg State Polytechnical University Journal. Physics and Mathematics.* 12 (2) (2019) 130–139 (in Russian).
6. **Jin Z.-H., Batra R. C.**, Interface cracking between functionally graded coatings and a substrate under antiplane shear, *Int. J. Eng. Sci.* 34 (15) (1996) 1705–1716.
7. **Li Y.-D., Lee K. Y.**, An anti-plane crack perpendicular to the weak/micro-discontinuous interface in a bi-FGM structure with exponential and linear non-homogeneities, *Int. J. Fract.* 146 (4) (2007) 203–211.
8. **Ding S.-H., Li X.**, Mode-I crack problem for functionally graded layered structures, *Int. J. Fract.* 168 (2) (2011) 209–226.
9. **Tikhomirov V. V.**, Stress singularity in a top of the composite wedge with internal functionally graded material, *St. Petersburg State Polytechnical University Journal. Physics and Mathematics.* (3) (225) (2015) 96–106 (in Russian).
10. **Jin Z.-H., Batra R. C.**, Some basic fracture mechanics concepts in functionally graded materials, *J. Mech. Phys. Solids.* 44 (8) (1996) 1221–1235.
11. **Tikhomirov V. V.**, Functionally graded wedge weakened by a semi-infinite crack, *St. Petersburg State Polytechnical University Journal. Physics and Mathematics.* 15 (3) (2022) 201–213 (in Russian).
12. **Noble B.**, Method based on the Wiener – Hopf technique for solution of partial differential equations. 2nd edition, American Mathematical Society, Washington, 1988.
12. **Noble B.**, Method based on the Wiener – Hopf technique for solution of partial differential equations, Pergamon Press, Oxford, 1958.
13. **Tikhomirov V. V.**, A semi-infinite crack of mode III in the bimaterial wedge, *St. Petersburg State Polytechnical University Journal. Physics and Mathematics.* (2 (242)) (2016) 126–135 (in Russian).



СПИСОК ЛИТЕРАТУРЫ

1. Wu X., Dzenis Y., Zou W. Screw dislocation interacting with an interfacial edge crack between two bonded piezoelectric wedges // International Journal of Fracture. 2002. Vol. 117. No. 3. Pp. 9–14.
2. Beom H. G., Jang H. S. A wedge crack in an anisotropic material under antiplane shear // International Journal of Engineering Science. 2011. Vol. 49. No. 9. Pp. 867–880.
3. Beom H. G., Jang H. S. A crack emanating from a wedge in dissimilar anisotropic materials under antiplane shear // International Journal of Fracture. 2012. Vol. 177. No. 2. Pp. 191–198.
4. Beom H. G., Jang H. S. Interfacial wedge cracks in dissimilar anisotropic materials under antiplane shear // International Journal of Engineering Science. 2012. Vol. 56. No. 1. Pp. 49–62.
5. Тихомиров В. В. Точное решение задачи для трещины, выходящей из вершины двух разнородных клиньев // Научно-технические ведомости СПбГПУ. Физико-математические науки. 2019. Т. 12. No. 2. С. 139–130.
6. Jin Z.-H., Batra R. C. Interface cracking between functionally graded coatings and a substrate under antiplane shear // International Journal of Engineering Science. 1996. Vol. 34. No. 15. Pp. 1705–1716.
7. Li Y.-D., Lee K. Y. An anti-plane crack perpendicular to the weak/micro-discontinuous interface in a bi-FGM structure with exponential and linear non-homogeneities // International Journal of Fracture. 2007. Vol. 146. No. 4. Pp. 203–211.
8. Ding S.-H., Li X. Mode-I crack problem for functionally graded layered structures // International Journal of Fracture. 2011. Vol. 168. No. 2. Pp. 209–226.
9. Тихомиров В. В. Сингулярность напряжений в вершине композитного клина с внутренним функционально-градиентным материалом // Научно-технические ведомости СПбГПУ. Физико-математические науки. 2015. No. 3 (225). С. 106–96.
10. Jin Z.-H., Batra R. C. Some basic fracture mechanics concepts in functionally graded materials // Journal of Mechanics and Physics of Solids. 1996. Vol. 44. No. 8. Pp. 1221–1235.
11. Тихомиров В. В. Функционально-градиентный клин, ослабленный полубесконечной трещиной // Научно-технические ведомости СПбГПУ. Физико-математические науки. 2022. Т. 15. No. 3. С. 213–201.
12. Noble B. Method based on the Wiener – Hopf technique for solution of partial differential equations. 2nd edition. Washington: American Mathematical Society, 1988. 246 p.
13. Тихомиров, В. В. Полубесконечная трещина моды III в биматериальном клине // Научно-технические ведомости СПбГПУ. Физико-математические науки. 2016. No. 2 (242). С. 135–126.

THE AUTHOR

ТИХОМИРОВ Victor V.

Peter the Great St. Petersburg Polytechnic University
29 Politechnicheskaya St., St. Petersburg, 195251, Russia
victikh@mail.ru

СВЕДЕНИЯ ОБ АВТОРЕ

ТИХОМИРОВ Виктор Васильевич – кандидат физико-математических наук, заместитель директора по образовательной деятельности Института прикладной математики и механики Санкт-Петербургского политехнического университета Петра Великого.

195251, Россия, г. Санкт-Петербург, Политехническая ул., 29
victikh@mail.ru

Received 17.03.2023. Approved after reviewing 14.05.2023. Accepted 14.05.2023.

Статья поступила в редакцию 17.03.2023. Одобрена после рецензирования 14.05.2023. Принята 14.05.2023.